Charge-pickup processes in relativistic heavy-ion reactions

K. Sümmerer,[1] J. Reinhold,[2] M. Fauerbach,[3,*] J. Friese,[2] H. Geissel,[1]
H.-J. Körner,[2] G. Münzenberg,[1] R. Schneider,[2] and K. Zeitelhack[2]
[1] *Gesellschaft für Schwerionenforschung, D-64220 Darmstadt, Germany*
[2] *Physikdepartment E12, Technische Universität München, D-85747 Garching, Germany*
[3] *Technische Hochschule Darmstadt, D-64289 Darmstadt, Germany*
(Received 31 March 1995)

We have measured a complete isotope distribution of projectile-like nuclear-charge pickup products, formed by bombarding a ^{27}Al target with 790A MeV ^{129}Xe ions. The shape of the cross-section distribution indicates a dominant influence of evaporation processes during the formation of the final cesium fragments observed, thus masking to a large extent the primary processes involved in the charge exchange. We can show, however, that an intranuclear-cascade-plus-evaporation calculation can reproduce the observed yields, and that the effect of Δ-formation during the first stage of the reaction is visible even in the inclusive cross sections. The same model can explain the strong increase in total charge-pickup cross sections with increasing projectile mass noted previously by other authors. It is therefore not necessary to invoke coherent processes to explain this increase as has been suggested previously.

PACS number(s): 25.75.+r, 25.70.Mn, 25.70.Kk

Nuclear charge-exchange reactions at relativistic energies ($E/A \gtrsim 500$ MeV) are of considerable current interest since they allow one to draw some conclusions on the in-medium behavior of pions and deltas. For heavy-ion-induced charge-exchange reactions, the most comprehensive study has been performed at the SATURNE accelerator at Saclay [1], with ^{40}Ar as the heaviest projectile. In these experiments, both the (n,p) and the (p,n) charge-exchange products were identified with respect to nuclear charge and mass at the SPES4 spectrometer. Two contributions to the charge-exchange process were clearly visible in the inclusive momentum spectra of the ejectiles: A narrow peak near zero momentum loss indicated the contribution from quasielastic isospin-exchange scattering, whereas a broader peak at an excitation energy of about 300 MeV was attributed to charge-exchange proceeding via Δ formation in the target.

For projectiles heavier than argon, neither production cross sections nor momentum spectra have been measured for individual charge-exchange products. The only information available up to now consists of total charge-pickup cross sections (summed over all isotopes with nuclear charge Z_p+1) measured for projectiles between ^{56}Fe and ^{197}Au at energies between 0.4A and 1.7A GeV (see Ref. [2] for a summary of the experimental situation). In some studies the product nuclear charge was measured with track detectors [3–5], in others with electronic detectors [2,6,7]. Since the mass of the fragments could not be measured, only little information on the reaction mechanism could be inferred from such studies. Nevertheless, Guoxiao *et al.* [3] found evidence for an increase of the total charge-pickup cross section that scales with the square of the projectile mass number, A_p, according to the empirical relation

$$\sigma_{\Delta Z=+1} = 1.7 \times 10^{-4} \gamma_{pt} A_p^2 \text{ mb}, \quad (1)$$

with

$$\gamma_{pt} = A_p^{1/3} + A_t^{1/3} - 1,$$

where the indices p and t refer to target and projectile, respectively. They claim that this dependence on A_p^2 is "the steepest ever reported for a nuclear process."

The present experiment makes use of the possibilities of the projectile-fragment separator FRS at GSI [8] to separate and identify mass-resolved charge-pickup products from heavy ions accelerated to relativistic energies by the SIS synchrotron. As part of a comprehensive study of fragment formation in the reaction of a 790A MeV ^{129}Xe beam with a ^{27}Al target [9], we have measured formation cross sections of several isotopes of $_{55}$Cs formed by charge pickup in $^{129}_{54}$Xe. The large incident energy kinematically focuses the reaction products completely into the FRS acceptance so that absolute formation cross sections can be determined. In principle, our setup allows one also to measure the momentum distributions of the fragments in the dispersive midplane of the separator and to obtain spectra similar to those measured at SATURNE. Such data, though with poor statistics, have been obtained with a thin ^{9}Be target for 500A MeV ^{86}Kr projectiles [10]. In the present experiment, however, which was directed at measuring small production cross sections, a thick ^{27}Al target was used, leading to poorer momentum resolution. We will show, however, that also the isotopic cross-section distribution allows one to draw conclusions with respect to the reaction mechanism. By comparing this distribution with the results of an intranuclear cascade (INC) calculation, more insight into the underlying physical processes can be obtained. In particular, we can study the A_p dependence of the charge-pickup process and see whether the calculation reproduces the quadratic dependence found in Ref. [3].

*Present address: NSCL, Michigan State University, East Lansing, MI 48824.

A ^{129}Xe beam with an intensity of about 10^8 ions per spill (every 5 s) was delivered from the heavy-ion synchrotron SIS and hit a ^{27}Al target of 0.8 g/cm^2 mounted in front of the FRS. Reaction products produced in this target were identified by measuring their velocities at the exit of the FRS in a ring-imaging Cherenkov counter [11,12]. In addition, the magnetic rigidity $B\rho$ and the energy loss ΔE of the fragments were measured in the central dispersive image plane of the FRS with an array of silicon detectors [9]. Calibration runs with the primary ^{129}Xe beam at various energies served to calibrate the velocity and ΔE measurements. The resolution obtained amounted to $\Delta Z = 0.43$ [full width at half maximum (FWHM)] and $\Delta M = 0.7$ amu (FWHM). The intensity of the primary beam was determined with the help of a secondary-electron transmission detector [13]. Formation cross sections of $_{55}$Cs isotopes were determined from the numbers of identified isotopes by correcting for the loss of fragments in the target and in other layers of matter due to secondary reactions, and for the dead time of the data acquisition system. Figure 1 shows the resulting cross sections for 12 Cs isotopes with nuclear masses between A=118 and A=129. Peak cross section range up to a few millibarns, which is not surprising given the total charge-pickup cross sections of a few tenths of millibarns measured for very heavy ions in previous experiments [2–6].

We will now try to reproduce the measured mass distribution with a simple model calculation. Since we deal with relativistic energies and very peripheral processes, an intranuclear-cascade calculation based on experimental free hadron-hadron cross sections should contain the essential physics. Multistep proton-transfer reactions that occur near the Coulomb barrier or in the Fermi energy domain can safely be excluded [14]. This is corroborated by the nonobservation of fragments with masses larger than A_p. We have used the intranuclear-cascade model ISABEL [15] since it accounts for the diffuseness of the nuclear surface, an aspect that we think is crucial for the very peripheral processes that we consider in the present study. ISABEL is a purely classical model with the Pauli principle introduced in a schematic way as the only quantum-mechanical ingredient. Nuclear-charge-exchange processes proceed in this model either via (n,p) charge-exchange collisions where a virtual charged pion is exchanged. This process is implicitly contained in the parametrization of the differential (n,p) cross sections used in ISABEL. The other possibility is the excitation and subsequent decay of a Δ resonance by which a projectile neutron changes its isospin.

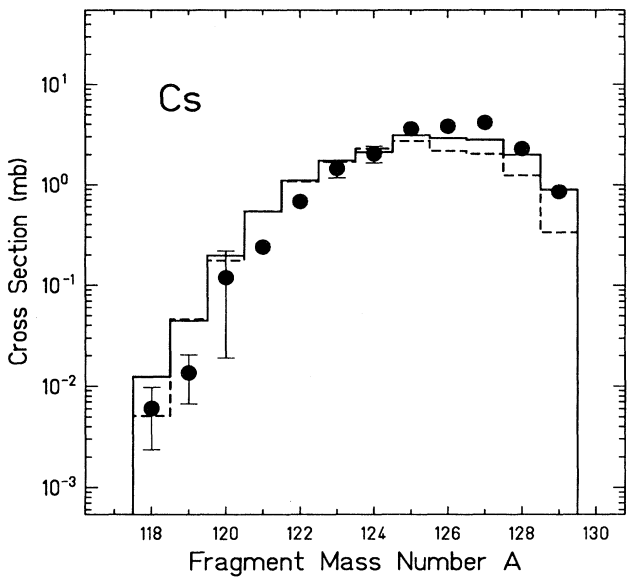

FIG. 1. Production cross-sections for cesium isotopes produced by nuclear-charge pickup in ^{129}Xe at $E = 790A$ MeV. The full histogram is the result of an intranuclear-cascade calculation with ISABEL and PACE (ISAPACE; see text). The dashed histogram was obtained by switching off Δ formation in the ISABEL calculation.

It is obvious that the intranuclear cascade normally produces excited prefragments that decay subsequently, mainly by neutron emission in our case, to the final fragments observed. To model this second step of the reaction, the evaporation code PACE has been coupled to the ISABEL model (ISAPACE, [15–18]). The full histogram in Fig. 1 shows the final fragment distribution after the evaporation step. The calculated curve reproduces well the height, position, and width of the experimental isotope distribution, though minor discrepancies can be observed near the maximum and on the neutron-deficient side of the distribution.

Our model calculations of the charge exchange tell us that in the INC step of the reaction, e.g., the prefragment ^{129}Cs is created via (n,p) charge-exchange scattering in about 55% of all cases, whereas Δ formation is involved in about 45% of all cases. As indirect evidence for the latter reaction mechanism we note that the resulting isotope distribution is altered — in particular for the pure charge exchange ^{129}Xe$\rightarrow^{129}$Cs — if we artificially suppress Δ formation in nucleon-nucleon collisions (dashed curve in Fig. 1).

We will now investigate if our model calculations can also explain the apparent strong increase of the total charge-pickup cross section with increasing projectile mass noted in Ref. [3]. We do this by comparing, in Fig. 2(b), our measured cross section for the system ^{129}Cs + ^{27}Al at 790A MeV ($\sigma_{\Delta Z=+1} = 19.3 \pm 0.8$ mb, obtained by integrating the mass distribution of Fig. 1) and those measured for other systems between ^{56}Fe + ^{27}Al and ^{197}Au + ^{27}Al [2,6,19] at incident energies between 0.62A and 1.57A GeV with results from our ISAPACE calculations. The numerical values of the data points, the references to the original literature, and the incident beam energies at which these data were taken are listed in Table I.

In using data taken at different incident energies in our comparison, we neglect a small energy dependence of the charge-pickup cross sections which has been shown to be rather weak between 500A and 1000A MeV both by experiments [2,4,6] and ISAPACE calculations [17]. We also do not consider very light nuclei like ^{12}C or ^{18}O since the small number of bound states in light nuclei hampers a comparison with heavy nuclei which have a large number

of bound states and are therefore more appropriate for a comparison with statistical models.

The good agreement between the experimental data points in Fig. 2(b) (circles) and the calculated ones from our ISAPACE calculations (squares) demonstrates that the model contains the essential physics that governs the increase of the charge-pickup cross sections with projectile mass. In particular the flat slope in the range $139 \leq A_p \leq 197$, where the measured charge-pickup cross sections increase proportional to $A^{1.02}$, is well reproduced. Also the striking difference between the cross sections for ^{56}Fe and ^{58}Ni is reproduced in the ISAPACE calculation: Since these projectiles are very close in mass, the empirical scaling law of Eq. (1) would predict also very similar charge-pickup cross sections, whereas measured (and calculated) cross sections differ by about a factor of 5. The reason for this behavior will be discussed in more detail below.

When interpreting these observations in terms of our ISAPACE model, we have to distinguish between effects that are due to the primary (INC) process and those due to evaporation from the excited prefragments. To illustrate the former effect, we plot in Fig. 2(a) the (unobservable) prefragment charge-pickup cross sections as calculated with ISABEL. The dotted line fitted to these points shows an approximately linear dependence on A_p. This slope is steeper than expected from a purely peripheral process which we expect to scale with $A_p^{1/3}$. Such a scaling has indeed been observed for fragmentationlike reactions, where nucleons are removed from the projectile. But in our case of charge pickup at least one scattered nucleon from a (n,p)-type reaction has to be reabsorbed by the projectile. The probability for reabsorbtion should scale approximately with the projectile area; therefore, $\propto A_p^{2/3}$. Thus a scaling proportional to $A_p = A_p^{1/3} A_p^{2/3}$ may be anticipated from simple arguments. In any case it is much flatter than the A_p^2 dependence of coherent processes discussed by Guoxiao *et al.* [3].

The final-fragment charge-pickup cross sections shown in the lower panel of Fig. 2 result from the statistical deexcitation of the charge-pickup prefragments formed in the INC step of the reaction. Neutron evaporation modifies the shape of the $Z_p + 1$ isotope distribution (see Fig. 1), but does not change the total charge-pickup cross section. Proton evaporation, on the other hand, depletes the prefragment cross sections. Given the (calculated) linear scaling of the prefragment cross sections proportional to A_p, this final step of the reaction obviously accounts for most of the variation of the charge-pickup cross sections with A_p. It is obvious that the high Coulomb barriers of heavy nuclei hinder proton evaporation much more than in the case of low-Z nuclei. This can be seen if one compares the survival probabilities (the ratios of fragment to prefragment cross sections, columns 5 and 6 in Table I) of charge-pickup products from ^{129}Xe, ^{139}La, ^{165}Ho, and ^{197}Au, which are calculated to be 55%, 64%, 66%, and 57%, respectively, with the corresponding number

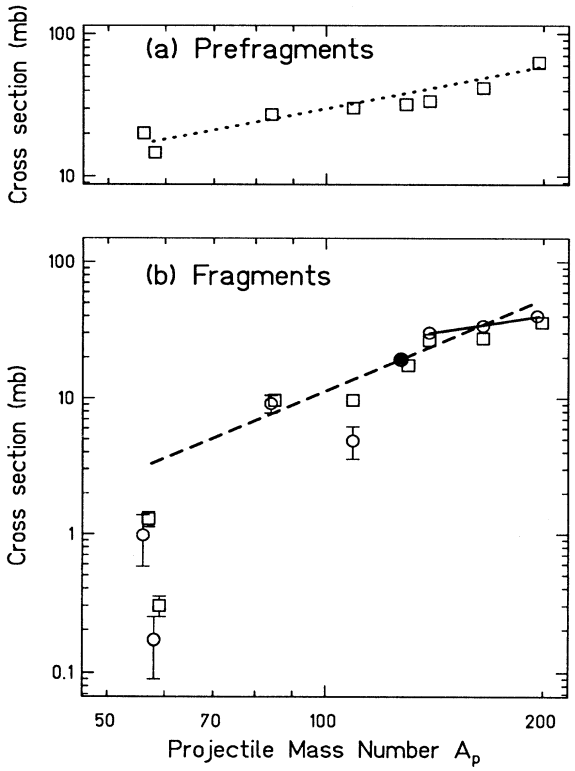

FIG. 2. Total cross sections for charge-pickup of relativistic projectiles using ^{27}Al targets at energies between $0.62A$ and $1.57A$ GeV, plotted as a function of the projectile mass number. (a) Prefragments (calculated results from ISABEL, prior to evaporation). The dotted line has been fitted to the data to demonstrate the approximately linear dependence on A_p. (b) Fragments (after evaporation). The solid symbol indicates the experimental data point from this work; the data shown with open circles have been taken from Refs. [2,6,19]. The open squares show the corresponding calculated cross sections from our INC+evaporation calculations with the code ISAPACE (see text). The solid line has been fitted to the heavy-mass experimental data, while the dashed line represents the empirical relation of Guoxiao *et al.* [3] proportional to A_p^2.

TABLE I. Measured vs simulated cross sections for charge-pickup reactions (ΔZ=+1) in ^{27}Al targets. The errors for the simulation are due to statistical uncertainties. As the fragment statistics was increased by using each prefragment 10 times in the evaporation cascade, the error for the fragment cross section is smaller than for that of the prefragment. The experimental value for ^{58}Ni has been measured with a ^{9}Be target [19] and scaled by a factor of 1.19 according to γ_{pt} in Eq. (1) for comparison with the other data points.

Proj.	$E_{\rm lab}$ [A GeV]	Ref.	Cross section [mb]		
			Experiment	ISASPACE calculation	
				Fragment	Prefragment
^{56}Fe	1.57	[6]	0.98 ± 0.40	1.29 ± 0.16	20.1 ± 1.2
^{58}Ni	0.65	[19]	0.17 ± 0.08	0.30 ± 0.05	14.7 ± 1.1
^{84}Kr	0.62	[2]	9.15 ± 1.36	9.66 ± 0.29	27.2 ± 1.4
^{109}Ag	0.93	[2]	4.88 ± 1.31	9.68 ± 0.32	30.2 ± 1.8
^{129}Xe	0.79	this work	19.3 ± 0.8	17.5 ± 0.2	32.1 ± 0.8
^{139}La	1.17	[6]	27.9 ± 2.4	21.7 ± 0.5	33.8 ± 1.9
^{165}Ho	0.77	[6]	33.9 ± 2.6	27.5 ± 0.9	41.7 ± 3.5
^{197}Au	0.92	[6]	40.1 ± 3.1	35.9 ± 1.4	63.0 ± 5.9

for ^{56}Fe, which is only 5%. The moderate increase in the (relative) magnitude of the Coulomb barrier for the heaviest projectiles studied explains also why the empirical relation of Guoxiao *et al.* [dashed line in Fig. 2(b)] overpredicts the measured charge-pickup cross section of ^{197}Au (the discrepancy, not clearly visible in the log-log representation of Fig. 2, amounts to 3.6 standard deviations).

When looking at nuclei with similar mass proton evaporation is hindered for more neutron-rich prefragments compared to more neutron-deficient ones due to the difference in proton binding energy. This explains the rather large difference for the two nuclei ^{56}Fe and ^{58}Ni. As expected, the prefragment cross sections for these projectiles with nearly equal masses are calculated to be very similar in magnitude [see Fig. 2(a)]. Since the ^{58}Ni prefragments are more neutron deficient than those from ^{56}Fe, however, more protons are lost during the evaporation stage, so that only about 2% of the charge-pickup prefragments survive evaporation, compared to about 5% in the case of ^{56}Fe.

We conclude that the present measurement of isotopically resolved charge-pickup cross sections for relativistic ^{129}Xe projectiles allows a more detailed comparison with model calculations than the previously available total charge-pickup cross sections. The experimental isotope distributions are well reproduced by simple intranuclear-cascade-plus-evaporation calculations based on free hadron-hadron cross sections in the framework of a purely classical model. Our model also predicts with good accuracy the projectile-mass dependence of total charge-pickup cross sections. The strong decrease observed for light projectiles is attributed to the lower Coulomb barriers of these nuclei, leading to correspondingly larger proton evaporation probabilities during the decay of the excited prefragments. The apparent scaling of the cross sections with A_p^2 noted previously is to a large extent fortuitious and does not reflect a primary process with such a strong A_p dependence. The basic nucleon-nucleon processes forming these prefragments are calculated to depend linearly on the projectile mass and do not require the assumption of coherent effects in the collisions. As the next step, it would be interesting to measure the momentum distributions for such charge-pickup products with very good accuracy and to see whether they agree with those of the ISABEL calculation. Thus one could check to which extent the assumption of free nucleon-nucleon reactions is valid.

The authors wish to thank K.-H. Behr, A. Brünle, and K. Burkard for technical assistance and Z. Fraenkel and S. Yasur for help with the code ISABEL. The authors are indebted to T. Blaich for providing his modified PACE code, to M. Cronqvist for an updated version of the ISAPACE package, and to B. Blank for providing unpublished data and critically reading the manuscript. Discussions with C. Bertulani, H. Lenske, W.F.J. Müller, T. Rubehn, and M. Roy-Stephan are gratefully acknowledged.

[1] C. Gaarde, Annu. Rev. Nucl. Part. Sci. **41**, 187 (1991), and references cited therein.
[2] B.S. Nilsen, C.J. Waddington, W.R. Binns, J.R. Cummings, T.L. Garrard, L.Y. Geer, and J. Klarmann, Phys. Rev. C **50**, 1065 (1994).
[3] Ren Guoxiao, P.B. Price, and W.T. Williams, Phys. Rev. C **39**, 1351 (1989).
[4] Jing Guiru, W.T. Williams, and P.B. Price, Phys. Rev. C **42**, 769 (1990).
[5] A.J. Westphal, Jing Guiru, and P.B. Price, Phys. Rev. C **44**, 1687 (1991).
[6] J.R. Cummings, W.R. Binns, T.L. Garrard, M.H. Israel, J. Klarmann, E.C. Stone, and C.J. Waddington, Phys. Rev. C **42**, 2508 (1990); **42**, 2530 (1990).
[7] W.R. Binns, J.R. Cummings, T.L. Garrard, M.H. Israel, J. Klarmann, E.C. Stone, and C.J. Waddington, Phys. Rev. C **39**, 1785 (1989).
[8] H. Geissel *et al.*, Nucl. Instrum. Methods Phys. Res. B **70**, 286 (1992).
[9] J. Friese, H.-J. Körner, J. Reinhold, R. Schneider, K. Zeitelhack, H. Geissel, A. Magel, G. Münzenberg, and K. Sümmerer, in *Proceedings of the 3rd International Conference on Radioactive Nuclear Beams*, East Lansing, Michigan, 1993, edited by D.J. Morrissey (Editions Frontieres, Gif-sur-Yvette, 1994); in *Proceedings of the 9th High-Energy Heavy-Ion Study*, Berkeley, California, 1993, edited by A.D. Chacon, M. Justice, and H.G. Ritter (University of California, Berkeley, 1994).
[10] K. Sümmerer *et al.*, in *Proceedings of the 3rd International Conference on Radioactive Nuclear Beams* [9].
[11] J. Friese *et al.*, in *Proceedings of the International Nuclear Physics Conference*, Wiesbaden, 1992 [Nucl. Phys. **A553**, 753c (1993)].
[12] K. Zeitelhack, J. Friese, H.-J. Körner, J. Reinhold, and R. Schneider, Nucl. Instrum. Methods Phys. Res. A **333**, 458 (1993).
[13] C. Ziegler, T. Brohm, H.-G. Clerc, H. Geissel, K.-H. Schmidt, K. Sümmerer, D. Vieira, and B. Voss, GSI Scientific Report 1990, Report GSI-91-1, 1991, p. 291.
[14] H. Lenske, H.H. Wolter, and H.G. Bohlen, Phys. Rev. Lett. **62**, 1457 (1989).
[15] Y. Yariv and Z. Fraenkel, Phys. Rev. C **20**, 2227 (1979).
[16] T. Blaich, M. Begemann-Blaich, M.M. Fowler, J.B. Wilhelmy, H.C. Britt, D.J. Fields, L.F. Hansen, M.N. Namboodiri, T.C. Sangster, and Z. Fraenkel, Phys. Rev. C **45**, 689 (1992).
[17] M. Fauerbach, thesis, TH Darmstadt, 1992.
[18] K.-H. Schmidt *et al.*, Nucl. Phys. **A542**, 699 (1992).
[19] B. Blank (private communication).